Final Report on the Large-Scale Production of Carbon Nanotubes Using the Jefferson Lab Free Electron Laser

submitted by:

Dr. Brian C. Holloway
Associate Professor
Department of Applied Science
College of William and Mary
PO Box 8795
Williamsburg, VA 23187-8795
(757) 221-3803
holloway@as.wm.edu

Account Number NCC-1-01056
May 1, 2001 – July 24, 2003

Abstract

We report on our interdisciplinary program to use the Free Electron Laser (FEL) at the Thomas Jefferson National Accelerator Facility (J-Lab) for high-volume pulsed laser vaporization synthesis of carbon nanotubes. Based in part on the funding of from this project, a novel nanotube production system was designed, tested, and patented. Using this new system nanotube production rates over 100 times faster than conventional laser systems were achieved. Analysis of the material produced shows that it is of as high a quality as the standard laser-based materials.

Since the first reports of the single-walled carbon nanotube (SWNT) in 1991 by researchers at NEC and IBM Almaden [1,2], different synthesis routes, such as the Arc Discharge (AD) [1-3], Pulsed Laser Vaporization (PLV) [4], and Chemical Vapor Deposition (CVD) [5-7] methods, have been developed to improve both the production rate and fractional conversion of the carbon feedstock to SWNTs. In the ensuing ten years since their discovery, catapulted forward by the pioneering PLV work at Rice University [4], SWNTs have been the subject of intense worldwide fundamental research and development [8]. The results of these previous efforts indicate that many applications for SWNTs can be contemplated, *if* higher production rates can be developed while maintaining the integrity of the tube wall. With the Jlab FEL, our preliminary experiments produced high quality SWNTs at 1.5 gm/h. This production rate is limited by the chamber design (mainly soot clearing and target temperature concerns) and not by the laser power. Assuming a linear scale up of production rate with laser power, full-power operation of the FEL would give a soot production rate of 4.5 gm/h. After the current Jlab FEL upgrade is complete, operation at a full power of 10 kilowatts could produce SWNTs at ~ 45 gm/h. It should also be noted that the system has not been optimized for wavelength or other parameters, suggesting that production rates over 45 gm/h are possible. For example, the FEL output can be tuned to absorption bands of gas phase species (e.g., C_2), which may alter significantly the reaction pathways.

We found that the ultrafast pulse structure of the FEL beam was critical to the production of high quality samples. Ultrafast ablation is sometimes referred to as "non-thermal," as the pulse duration is short relative to the time required for the heat wave to penetrate the target. This results in little collateral melting around the ablation spot.

When we deliberately melted the target with the FEL beam, SWNTs production dropped significantly. To achieve the high quality samples analyzed here, conditions were adjusted (target spin rate and laser flux) so that material removal beyond the confines of the laser spot was not observed.

Built, in part, to demonstrate a novel energy recovery method that dramatically increases efficiency [9,10], the 1 kW Jefferson Lab is currently 100 times more powerful than other existing FEL's, and 1000 times more powerful than tabletop sources of ultrafast laser light which typically are limited to a few watts [11].

A necessary requirement for the production of SWNTs found by all routes investigated so far appears to be the presence of small metal particles that can be found at an end of an individual tube or bundle of nanotubes. The growth mechanism may well be the Vapor-Liquid-Solid mechanism proposed for filament growth, where the filament is a surface precipitate from a carbon-saturated metal particle [12]. If the particle diameter is small enough ($d < 4$ nm)[13], individual tubes are observed; larger metal particle sizes ($d \sim 10 - 20$ nm) seem to produce bundles of aligned SWNTs that are held together by van der Waals forces. Multiwall carbon nanotubes (i.e., many SWNTs in a nested concentric array) can be produced by CVD with even larger diameter particles [14]. Synthesis routes that utilize the vaporization of carbon, i.e., AD and PLV, incorporate the required metal directly into the carbon feedstock. Metal, or metal carbide particles presumably form by condensation from the metal-carbon vapor. On the other hand, chemical vapor deposition (CVD) methods utilize pre-existing metal particles (supported [5, 7], or unsupported [6]) that may also act as a dehydrogenation catalyst converting hydrocarbon gases into the carbon feedstock at the particle surface. In the present case, Ni-Y and Ni-

Co were both added at 1 - 4 at. % to graphite powder and pressed into long 2.5 cm diameter carbon rods (CarboLex, Inc). Both the Ni-Y and No-Co catalysts produced high yields of tubes of similar quality and diameter distribution. This is interesting, because the prevailing literature suggests that Ni-Y [3] and Ni-Co[4] are, respectively, optimal catalysts for arc discharge (AD) and pulsed laser vaporization (Nd:YAG) growth. In the 3 micron wavelength FEL beam, both catalysts worked equally well.

Figure 1 shows a schematic of the experimental setup used at the Jlab FEL in the present experiments. The growth chamber is a fused quartz "T" constructed from a 50 mm diameter tube with a 25 mm diameter side-arm. The 50 mm tube is centered in a 1 meter long, split tube-furnace, and the side-arm protrudes out the side of the furnace near the center of the hot zone. Incident FEL radiation passes through a CaF_2 optical window on the end of the side arm and strikes a catalyzed carbon rod (target) mounted on a rotating and translating quartz rod, as shown in Fig. 1. A jet of pre-heated (1000 °C) argon exits through a ~ 0.4 mm diameter hole in a nozzle tip situated 6 mm off the rotating target surface, and about 1 cm upstream from where the laser spot strikes the target. The Ar gas jet deflects the ablation plume almost 90^0 away from the incident FEL beam direction, clearing away the carbon vapor from the region in front of the target. This "side-pumped" geometry was developed after we discovered that the conventional front-pumped counterflow PLV geometry was ill suited for our high target ablation rate. In the current work reported here, an overall Ar flow rate of 400 sccm in the 50 mm tube at 500 Torr was maintained by electronic flow controller and pressure controller. The pressure variation was less than ±10 Torr during normal conditions, but could rise by as

much as 50 Torr during high laser power experiments. SWNT soot was collected from a water-cooled copper cold finger at the exhaust end of the 50 mm quartz tube.

For the production of the samples reported here, the Jlab FEL was operated at a repetition rate of 74.8 MHz with a pulse width of ~400 femtoseconds and an average power of 800 W. Due to optical transport losses, we estimate that only 500 W was incident on our target. The 500 W beam was mechanically shuttered at a 20% duty cycle (1 second on, 4 seconds off) to limit the heating of the target, yielding an actual average power of about 100 W. Target heating was monitored with a CCD camera which viewed the ablation zone through the last FEL beam turning mirror, a hard reflector at 3 μm with about 50 % transmission in the visible. The FEL beam was focussed with a 50 cm focal length CaF_2 lens to a spot size of ~100 μm, yielding a peak laser flux of ~5x 10^{11} W/cm^2, which is about 1000 times greater than the flux used in typical Nd:YAG based SWNT PLV systems [4]. Such a tight focus was required to reach the target ablation threshold, as each FEL pulse is only 1/200,000 as long as the typical 10 ns Nd:YAG pulse and carries proportionally less energy. However, at 74.8 MHz the FEL pulses arrive every 13 ns, delivering 7.5 million pulses for each single pulse delivered by a traditional 10 Hz Nd:YAG system.

Qualitatively, heating of the target could be monitored by the color temperature of its surface. Early results showed that excessive bulk target temperature produced poor quality samples, presumably because material was removed by melting and/or thermal vaporization rather than ultrafast ablation of precursors through the highly energetic laser-induced plasma plume. This is shown in figure 2 a, b, where images of a target surface exposed to 30 msec windows of laser radiation are displayed. The target was

translated (rotated) relative to a fixed laser beam in the direction indicated by the white arrows. In the Fig2a, we see well defined slot being cut in the target, whereas in Fig 2b poorly defined craters are observed when the laser flux (W/cm^2) was increased by a factor of five (5X). For practical reasons, we refer to target ablation in Fig 2a and 2b, respectively, as "non-thermal" and "thermal" ablation, consistent with the collateral damage evident in Fig 1b that we suggest is due to thermal effects. We realize this terminology, strictly speaking, requires extensive experiments to justify. Putting arguments about "thermal" or "non-thermal" ablation terminology aside, ablation conditions producing target "cutting" such shown in Fig 1a generated significantly better SWNT soot (higher carbon % in SWNT). Target heating, of course, was also influenced by the speed at which the target was rotated and translated along its axis. By trial and error, a target rotation rate was found (1.7 revolutions/sec) which gave a high "cutting rate" without producing collateral (thermal) damage around the ablation zone.

For the samples that were carefully characterized and reported here, the FEL wavelength was nominally 3 μm. Although we did not fine tune the laser wavelength in search of absorption features (e.g., C_2), we did attempt to synthesize SWNT's at other nominal wavelengths, specifically 1 μm, 5 μm and 6 μm. The FEL optics were not optimized for 1 and 5 μm, and at the resulting reduced power (~100 watts) we were unable to reach the ablation threshold of our target. At 6 μm we had high power, but we were unable to achieve non-thermal ablation, i.e. the target always showed melt debris on the surface. We suggest that at this longer wavelength, Debye shielding may have reflected much of the laser power, or that the target was heated by energy absorbed in the plasma plume rather than directly by the beam.

Sample characterization was carried out using SEM, AFM, TEM, TPO and Raman scattering, as mentioned above. SEM micrographs were taken using a JEOL JSM 5400 operating at 20KV. Samples were first coated with a thin film of Au to prevent charge accumulation. An SEM images (e.g., Fig.3) for the carbon soot produced with NiCo catalyst show long randomly oriented filaments (i.e., bundles). From TEM images we found, the bundle diameters ranged from ~4 - 10 nm for NiY-derived tubes, and larger bundles ~4 - 18 nm for NiCo-derived tubes. The metal content in the soot was determined by temperature-programmed oxidation (TPO) to be almost the same as the composition of the target [15]. The metal appears in low-resolution TEM images primarily as carbon-coated metal particles from a few nm to ~20 nm in diameter. AFM was used to investigate the lengths of the SWNT bundles produced by the FEL. Images were collected with a Nanoscope III (Digital Inst. Inc.) by dispersing the SWNT soot in ethanol with an ultrasonic horn (Misonix XL2020) for 5 min, and then placing a drop of the ethanol suspension on a freshly cleaved mica substrate. When the ethanol had almost evaporated the surface was blown by dry N_2 gas. The AFM images showed that the bundles were quite long. Typical lengths were in the range 5-20 microns. High resolution transmission electron microscopy was carried out in a JEOL 2010F (at 100 KV to minimize beam damage) to better reveal the structure of the SWNTs, nanocarbons and metal nanoparticles in the soots. Figure 4 (a, b) show high resolution TEM (HRTEM) images of SWNTs produced by using NiY and NiCo catalyst particles, respectively. The number of tubes within a typical bundles varies from 8 to ~200, although we observed many isolated SWNTs in soot produced with both catalysts. From HRTEM images, the individual SWNT diameter ranged from ~1-1.4 nm. Occasionally, HRTEM images show

the presence of peapod structures[16] (Fig. 4b). Fullerenic carbon shells are also observed outside of the SWNTs (Fig 4a, b). None of the HRTEM images revealed the presence of double-walled nanotubes (DWNT) or multi-walled nanotubes (MWNT). In the HRTEM images Fig. 4 (a, b), isolated SWNTs can be seen with perfectly hemispherical fullerenic caps.

Raman scattering spectra of carbon soots can provide the molecular fingerprint of the SWNT [17-18]. The first Raman spectra of SWNTs were recognized as being due to a resonant scattering process [18]. Later work identified the resonant Raman scattering with absorption between singularities in the electronic density of states due to the one-dimensional character of the SWNT [17]. Since the electronic density of states of the SWNT is diameter-dependent, different laser excitation frequencies excite tubes with different diameters (i.e., only a subset of the tubes can be excited with a single wavelength excitation)[17,19]. The spectra in Fig. 5 (a, b) were taken on soots derived from NiY and NiCo, respectively; four different excitation wavelengths were used (1064 nm, 647.0 nm, 514.5 nm, 488.0 nm) to sample, via diameter-selective resonant scattering, four different subsets of tubes in the sample. The visible Raman spectra were collected at room temperature in the backscattering configuration using a JY-ISA T64000 spectrometer with an Olympus BH3 confocal microscope (~1 μ diameter focal spot), whereas the IR Raman spectrum using 1064 nm excitation was taken with a BOMEM DA3+ FT-Raman spectrometer. Both spectrometers operated with a spectral slitwidth less than 1 cm^{-1}.

The Raman spectra of SWNTs are well known to exhibit two strong first-order features: the radial displacement band (radial breathing mode, ω_r), typically found in the

region 140-300 cm^{-1} and a tangential displacement band with maximum intensity near 1590 cm^{-1} that is relatively independent of tube diameter[19]. A somewhat broad, disorder-induced Raman band (or "D-band") in sp^2 carbon is usually observed in the region 1260-1350 cm^{-1}. This feature is known to be "dispersive" [20] and is common to all disordered sp^2 carbon materials. A "dispersive" mode is one whose Raman frequency changes with the excitation frequency. This dispersive character is a sign that the wave vector for these modes is not associated with the zone center (q=0). The D-band feature is very weak in our spectra and is indicate by a downpointing arrow in the spectrum. The D-band strength can either be identified with wall disorder in the SWNTs, or to scattering from sp^2 carbon nanoparticles, or to the presence of a carbon coating on the outside of the tube bundles. The fact that the D-band is weak in the spectra of Fig. 5 suggests that the fraction of disorderedsp^2 carbon in forms other than SWNTs is low in our samples, and that the wall disorder in the nanotubes is also low [7]. The Raman-active radial breathing mode is a clear spectroscopic signature of the cylindrical seamless SWNT, and the diameter-dependence of the mode frequency has been shown to be approximated by ω_r= (224 cm^{-1}. nm)/d(nm) + Δ, where Δ~12 cm^{-1} is the correction due to the tube-tube interaction within a bundle [19]. We have used this ω vs. d relation to add a SWNT diameter scale above the respective radial breathing mode regions in Fig. 5 (a, b). It should also be noted that the different shape of the tangential displacement bands (~ 1590 cm^{-1}) in Fig. 5 (a, b) under 647.1 excitation is due to the fact that primarily metallic tubes are being excited at this wavelength in these soots. This observation has been reported previously for PLV and AD materials, and stems from the nature of the metallic density of states, and the line broadening and shifting due to the electron-phonon interaction [19].

In the Fig. 5, the relative intensities of the tangential and radial bands in vary from one spectrum to the other. This is the result of the details of the resonant Raman cross section. For some excitation frequencies, the radial modes are more strongly enhanced than with others.

It should be noted that, the diameter distributions of the NiY- and NiCo-derived tubes, as revealed by their radial breathing mode frequencies, are remarkably similar. Furthermore, the Raman line widths for both the radial and tangential bands in both the NiY- and NiCo-derived samples are comparable, an indication of similar wall integrity in both samples.

Summarizing, electron microscopy and Raman Scattering both indicate that high quality SWNT bundles have been produced by ultrafast ablation using the high power FEL at the Thomas Jefferson National Accelerator facility using a novel, patented, nanotube production system.

Project Output

Refereed Publications

- P. C. Eklund, B. K. Pradhan, U. J. Kim, Q. Xiong, J. E. Fisher, A. D. Friedman, B. C. Holloway, K. Jordan, M. W. Smith "Large-scale Production of Single-Walled Carbon Nanotubes Using Ultrafast Pulses From a Free Electron Laser", *Nano Letters*, 2 (2002) 6, 561-566.

Relevant Patents

- "Synthesis of Carbon Nanotubes Using High Average Power Ultra-fast Laser Ablation", disclosure filed Jan 2002.

Invited Talks

- "The Effect of Photon Energy, Average Power, and Repetition Rate on Nanotube Synthesis Using a Free Electron Laser" XXIV National Meeting of the Brazilian Vacuum Society, Bauru, Sao Paulo, Brazil, July 2003
- "Carbon Nanotube Synthesis with the Jefferson Lab Free Electron Laser", Virginia Academy of Sciences Annual Meeting, Univ of Virginia, Charlottesville, VA, May 2003
- "Processing and Characterization of Carbon-Based Materials", University of Florida, Jan 2003
- "The Effect of Photon Energy, Average Power, and Repetition Rate on Nanotube Synthesis Using a Free Electron Laser" 12th National Meeting of the Mexican Vacuum Society, Veracruz, Mexico, Oct 2002
- "Carbon-based Materials – CN_x, DLC, and CSWNT", IV Brazilian Meeting and 33rd IUVSTA Workshop on Diamond, Diamond-like, Nanotubes, Nitrides and Silicon Carbide, Nov. 2001 ***(not presented due to death in family)***
- "This Is Not Your Parent's Idea of Carbon", Renneseler Polytech Institute, Oct 2001

Contributed Presentations

- "Carbon Nanotube Synthesis With The Jefferson Free Electron Laser", *Jefferson Lab Laser Processing Consortium Meeting*, Newport News, VA (talk presented March 2003)
- "Recent Advances in Nanotube Synthesis Using the Jlab FEL", *Jefferson Lab Laser Processing Consortium Meeting*, Newport News, VA (talk presented Jan. 2002)
- "The Effect of Photon Energy, Average Power, and Repetition Rate on Nanotube Synthesis Using a Free Electron Laser", *IUVSTA 15th International Conference*, San Francisco, CA , Oct 2001
- "Production of Single Walled Carbon Nanotubes Using Tunable Radiation From A Free Electron Laser (FEL)", *Carbon 2001*, Lexington, KY (talk presented by Peter Eklund, July 2001)

References

1. S.Iijima, T.Ichihashi, *Nature* **363**, 603 (1993)
2. D.S. Bethune *et al.*, *Nature* **363**, 605 (1993).
3. C.Journet *et al.*, *Nature* 388, 756 (1997).
4. A. Thess *et al.*, *Science* **273**, 483 (1996).
5. H. Dai, *et al.*, *Chem. Phys. Lett.* **260**, 471 (1996), A. M. Cassell, J. A. Raymakers, J. Kong, H. Dai, J.Phys.Chem.B, **103**, 6484 (1999).
6. P. Nikolaev *et al., Chem. Phys. Lett.* **313**, 91 (1999).
7. A. R. Harutyunyan, B. K. Pradhan, U. J. Kim, G. Chen and P. C. Eklund, *Nano Letters*, **3**
8. K. Tanaka, T. Yamabe, K. Fukui, *The Science and Technology of Carbon Nanotubes*, Elsevier, (Oxford, 1999); M. S. Dresselhaus, G. Dresselhaus, P. C.Eklund, Science of Fullerenes and Carbon Nanotubes; Academic Press: San Diego, 1996
9. R. W. Warren *et al.*, *Nucl. Instrum. Methods Phys. Res. Sect*; **A 237**, 180 (1985).
10. G. R. Neil, *et al.*, *Phys. Rev. Lett.* **84**, 662 (2000).
11. Decommissioned in November of 2001 to make way for an upgrade, the 1 kW FEL will be replaced by a nominal 10 kW system slated to come on line in late 2002. For more information on the Jlab FEL, readers are directed to (www.jlab.gov/FEL) and S. V. Benson et al., "Jefferson Lab Free-Electron Laser Starts Operation with Sustained Lasing at the Kilowatt Level," Synchrotron Radiation News, Vol. 13 (4) (July/August 2000).
12. G. G. Tibbet, J. Cryst. Growth, **73**, 431, (1985).

13. J. H. Hafner, C-L. Cheung, T. H. Oosterkamp, C. M. Lieber, J. Phys. Chem. B., **105**, 743, (2001)

14. M. Endo *et al.*, *Carbon*, **33**, 873, (1995).

15. The residual catalyst in the SWNT reaction product material was determined by temperature-programmed oxidation (TPO) using a thermogravimetric analyzer (TGA, IGA-3 Hiden UK). In this analysis, all the carbon is assumed converted to CO/CO_2, and the metal is converted to an oxide. Within the TGA, the carbon SWNT material to be analyzed for metal was maintained in a flow of dry air at 100 sccm, while the temperature was ramped linearly in time (5°C/min) from 25-1000°C.

16. B. W. Smith, M. Monthioux, D. E. Luzzi, *Nature*, **396**, 323 (1998).

17. A. M. Rao *et al.*, Science, **275**, 187 (1997).

18. J. M. Holden, *et al., Chem. Phys. Lett.*, **220**, 186 (1994).

19. M. S. Dresselhaus, P.C. Eklund, *Advances in Physics* **49**, 705 (2000).

20. A. K. Sood, R. Gupta and S. A. Asker, *J. Appl. Phys.*, **90**, 4449 (2001)

Figure Captions:

Figure 1. Schematic of the interaction geometry between the infrared ultrafast pulsed radiation from the FEL (0.5 ps pulses; 75 MHz repition rate, ~ 1 kWatt maximum average power) and the carbon/metal target. The target is a composite rod (e.g., graphite plus a few at% NiY or NiCo) that is rotated and translated while being ablated by the FEL beam. Pre-heated Ar gas is used to clear away the nanotubes from the FEL beam path.

Figure 2. Optical images of target surface exposed to 30 msec of laser radiation (a)"non-thermal" ablation and (b) "thermal" ablation.

Figure 3. Scanning Electron Microscope (SEM) images of bundles of "as-prepared" SWNTs produced with Ni/Y (1.0 at%/4.0 at%).

Figure 4. High Resolution Transmission Electron Microscopy (HRTEM) of "as-prepared" SWNT soot supported on a holy carbon grid, produced with (a) NiY catalysts and (b) NiCo catalysts.

Figure 5. Unpolarized Raman spectra of FEL SWNT soot collected at room temperature: (a) NiY catalysts and (b) NiCo catalysts. The spectra were collected in air under ambient conditions using 1064, 647.1, 514.5, and 488.0 nm radiation.

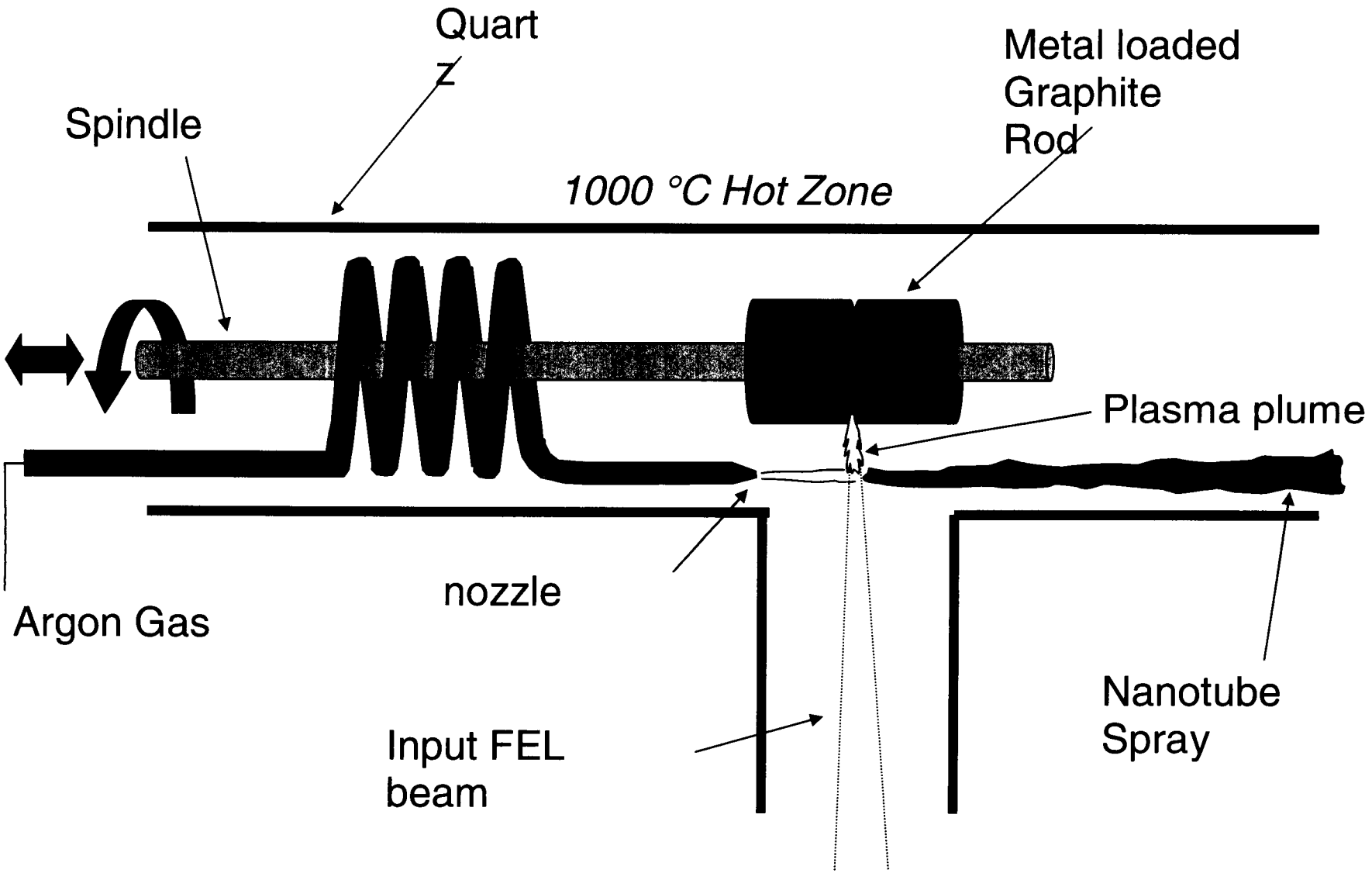
Quart
z
Spindle
Metal loaded
Graphite
Rod
1000 °C Hot Zone
Plasma plume
nozzle
Argon Gas
Input FEL
beam
Nanotube
Spray

Figure 1

(a)

(b)

Figure 2 (a) and (b)

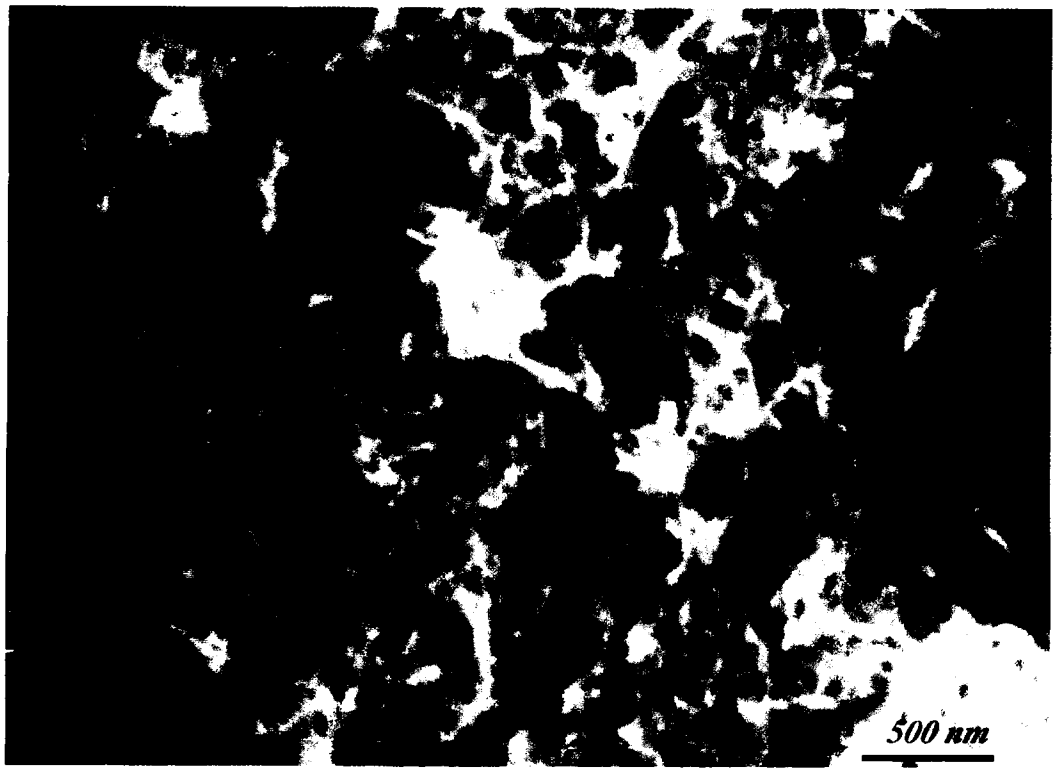

Figure 3

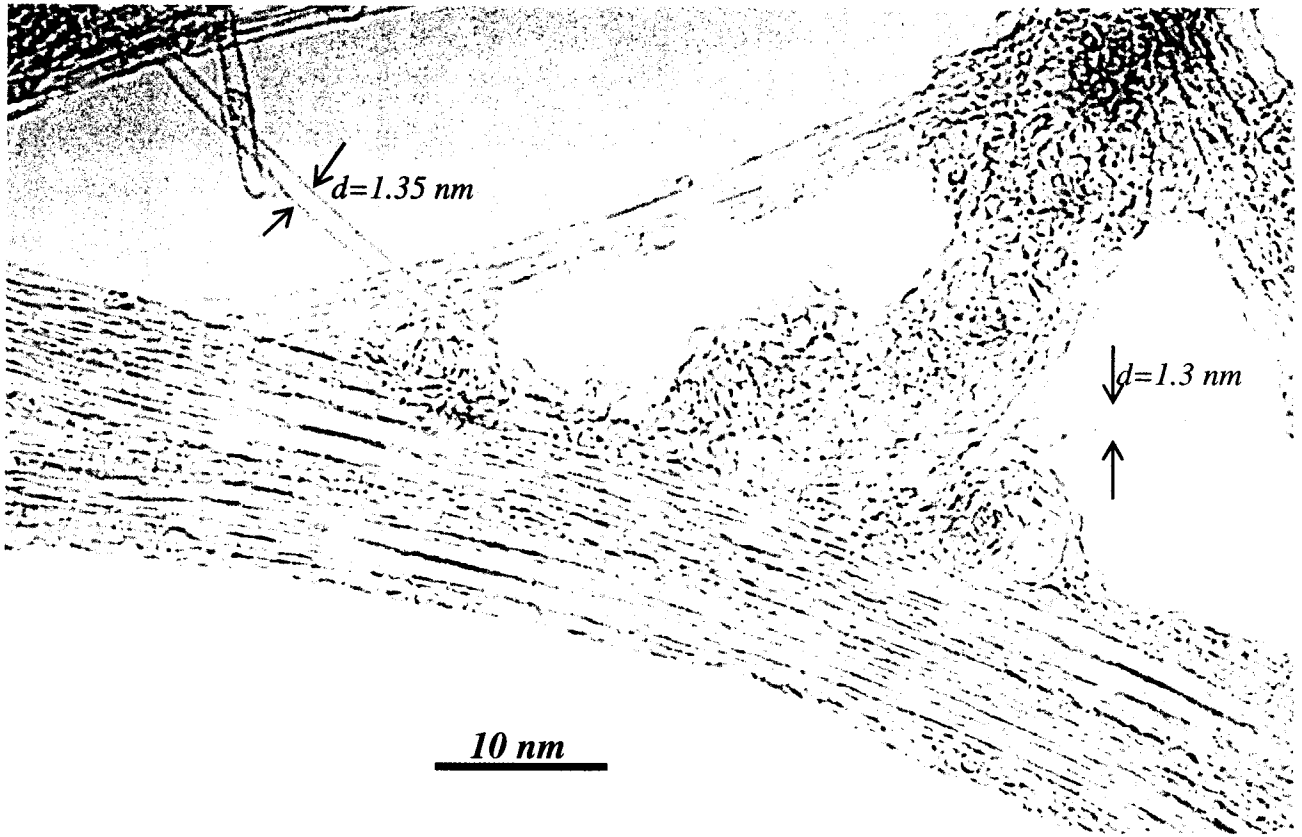

Figure 4 (a)

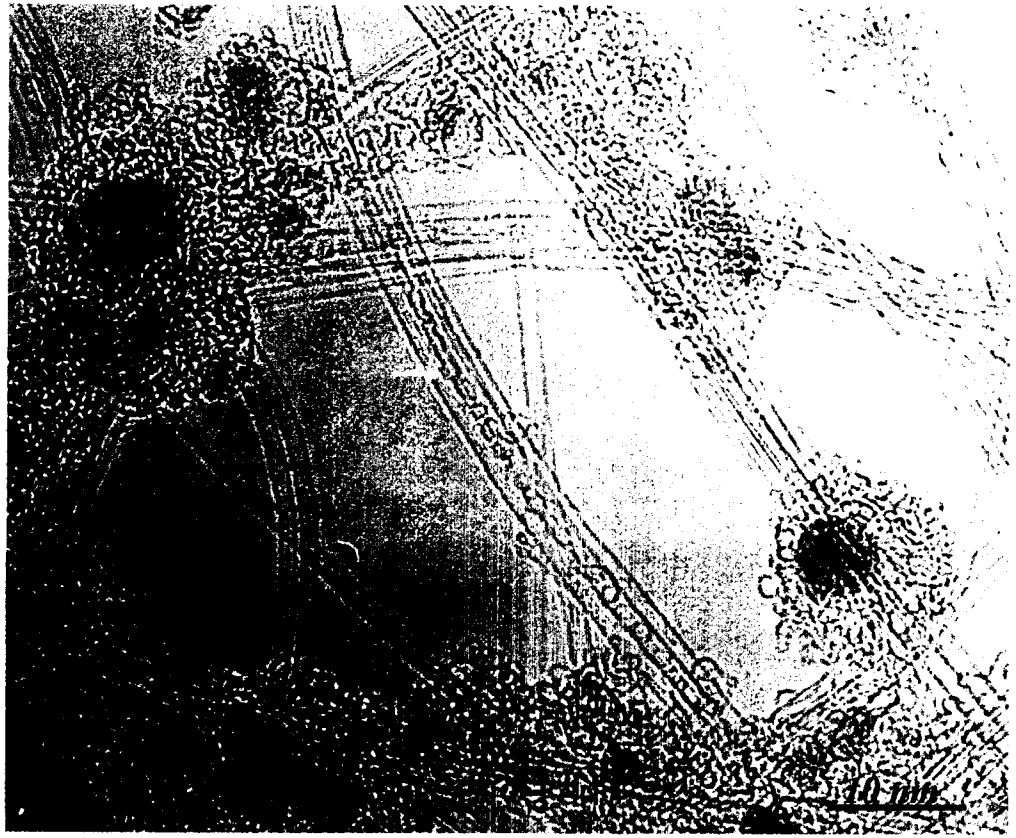

Figure 4 (b)

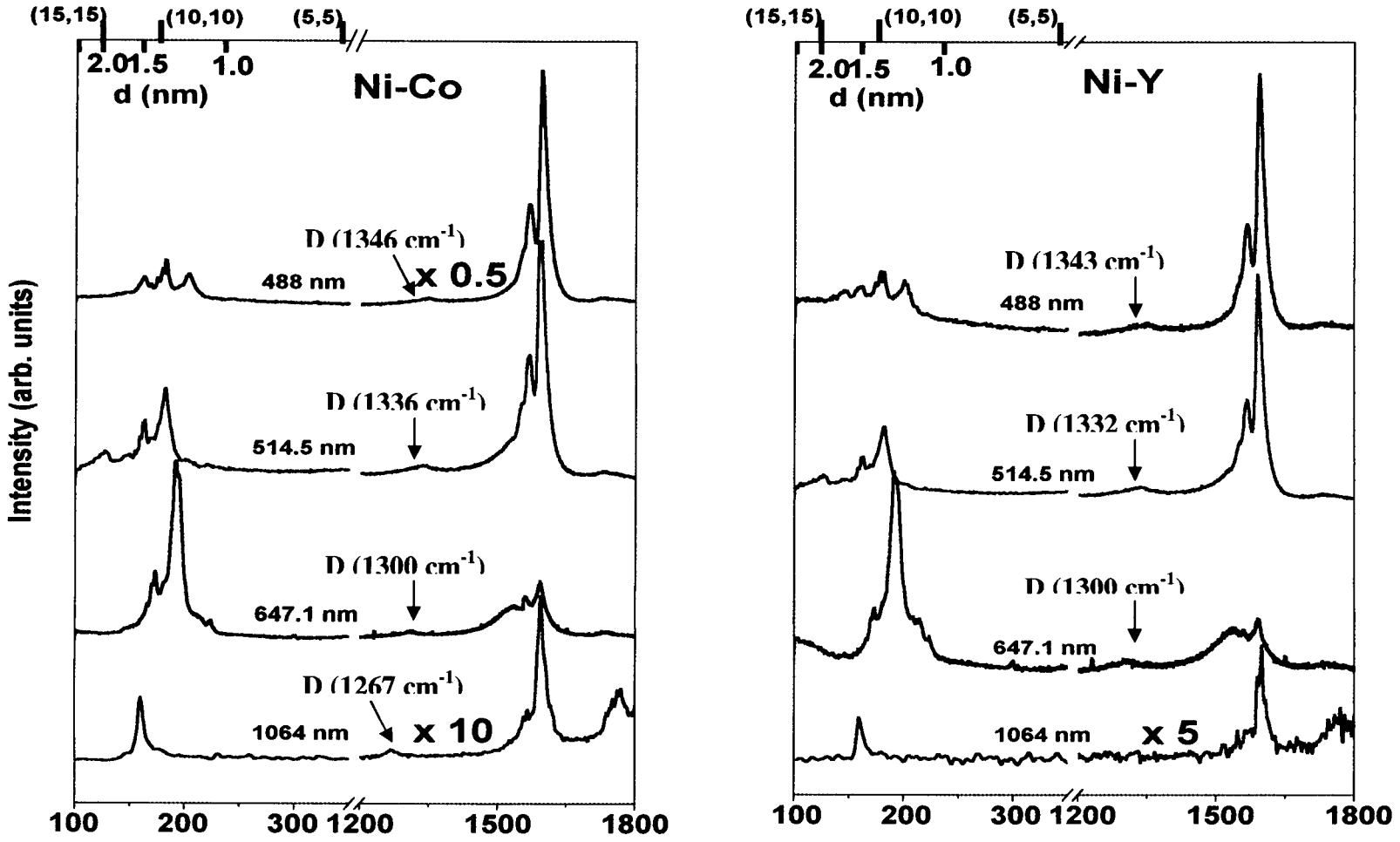

Figure 5 (a) and (b)